Brain Topogr (2012) 25:20–26
DOI 10.1007/s10548-011-0189-7

ORIGINAL PAPER

EEG Microstates During Resting Represent Personality Differences

Felix Schlegel · Dietrich Lehmann · Pascal L. Faber · Patricia Milz · Lorena R. R. Gianotti

Received: 28 February 2011 / Accepted: 23 May 2011 / Published online: 5 June 2011

Abstract We investigated the spontaneous brain electric activity of 13 skeptics and 16 believers in paranormal phenomena; they were university students assessed with a self-report scale about paranormal beliefs. 33-channel EEG recordings during no-task resting were processed as sequences of momentary potential distribution maps. Based on the maps at peak times of Global Field Power, the sequences were parsed into segments of quasi-stable potential distribution, the 'microstates'. The microstates were clustered into four classes of map topographies (A–D). Analysis of the microstate parameters time coverage, occurrence frequency and duration as well as the temporal sequence (syntax) of the microstate classes revealed significant differences: Believers had a higher coverage and occurrence of class B, tended to decreased coverage and occurrence of class C, and showed a predominant sequence of microstate concatenations from A to C to B to A that was reversed in skeptics (A to B to C to A). Microstates of different topographies, putative "atoms of thought", are hypothesized to represent different types of information processing.The study demonstrates that personality differences can be detected in resting EEG microstate parameters and microstate syntax. Microstate analysis yielded no conclusive evidence for the hypothesized relation between paranormal belief and schizophrenia.

F. Schlegel (✉) · D. Lehmann · P. L. Faber · P. Milz
The KEY Institute for Brain-Mind Research, University Hospital of Psychiatry, POB 1931, 8032 Zurich, Switzerland
e-mail: felix.schlegel@alumni.ethz.ch

L. R. R. Gianotti
Social and Affective Neuroscience, Department of Psychology, University of Basel, 4003 Basel, Switzerland

Keywords Microstate syntax · Cognition · Paranormal beliefs · Schizotypy · Transition probabilities · Schizophrenia

Introduction

The functional state of the brain changes continually, even if there are no stimuli or tasks. The brain's processing of a given, external or internal information depends on the momentary functional state. Brain state can be monitored by electroencephalography (EEG) at the split-second speed needed for successful interaction with the surround.

Multichannel EEG displayed as sequence of momentary potential topographies (maps) shows quasi-stable configurations (mean duration of about 100 ms for spontaneous EEG) called functional microstates (Lehmann et al. 1987) that are concatenated by rapid transitions. Different microstates have been attributed to different types of cognitive processes (Britz et al. 2009; Lehmann et al. 1998, 2010; Mohr et al. 2005; Müller et al. 2005) qualifying them for "atoms of thought" (Lehmann et al. 2010). Microstate topographies during no-task resting can be clustered into four map configurations that explain >80% of the total data variance (Koenig et al. 2002). These four classes have been observed in independent studies with notable similarity across subjects (Koenig et al. 1999; Lehmann et al. 2005). Microstate parameters (duration, frequency of occurrence) of the four classes differ between schizophrenics and controls (Irisawa et al. 2006; Kikuchi et al. 2007; Koenig et al. 1999; Lehmann et al. 2005). The temporal concatenation of microstates ('syntax') showed non-random behavior in healthy participants (Wackermann et al. 1993). Also, microstate syntax exhibited a particular, deviant pattern in untreated schizophrenics compared to controls

(Lehmann et al. 2005). Thus, the syntax of microstates may reflect personal cognitive strategies.

The EEG microstate concept was supported by fMRI studies where the time courses of microstates when convoluted with the hemodynamic response allowed to predict the BOLD signatures of resting-state networks ('RSNs') (Britz et al. 2010; Musso et al. 2010) which display slower spontaneous fluctuations (about 10 s for no-task conditions) of the coherences of the BOLD response (Mantini et al. 2007); microstates were thus suggested to represent the underlying electrophysiological basis of RSNs. This is due to the monofractal, scale-free dynamics of microstate sequences, i.e., the information contained in the temporal dynamics of microstates is preserved over large timescales (Van De Ville et al. 2010).

Inspired by the universality of EEG microstates, we wondered whether personality features of healthy people were also reflected in the parameters and syntax of microstates.

Using a previously obtained dataset (Pizzagalli et al. 2000), we examined microstates during spontaneous awake no-task resting EEG of participants who differ in their belief in paranormal phenomena.

Materials and Methods

352 university students answered a questionnaire (4-point scale) about belief in and experience of paranormal phenomena (Mischo et al. 1993). 117 agreed to participate in a subsequent EEG recording. Because 91 of the volunteers were women, men were excluded from the further assessment to avoid gender as a confounding factor. The questionnaire consists of 6 items, concerning mainly telepathy and precognition, and results in a score from 0 (strong skepticism) to 18 (strong belief in paranormal phenomena). Volunteers in the upper and lower 33% of the paranormal belief scale were accepted if right-handed, and native German speakers without personal or family history of psychiatric disorders. 19 'believers' and 18 'skeptics' remained for recordings. Eight persons with <10 s artifact-free EEG had to be excluded, leaving 16 believers (score range 15–18) and 13 skeptics (score range 0–6) for analysis. The two groups of participants did not differ in age, handedness and education level.

The study protocol was approved by the local Ethics Committee. Participants gave their written consent and were financially compensated.

Thirty-five EEG electrodes referenced to Cz were attached according to the 10–10 system (Chatrian et al. 1988). Electrodes at the outer left and right canthus and infraorbital monitored eye movements. Participants were comfortably seated in a sound- and light-shielded recording chamber. They were told that the recording will be done during no-task resting with closed or open eyes, requested via intercom, consisting of 20 s eyes open; 40 s eyes closed; 20 s eyes open; 40 s eyes closed. EEG was continuously recorded with 0.05–60 Hz band pass, digitized at 250 samples/s/channel. Only eyes closed recordings were used for analysis.

Eye movement artifacts were removed using ICA (BrainVision Analyzer 2.0, Brain Products, Munich, Germany), followed by careful manual screening for other artifacts using most conservative criteria. No further artifact correction was done (not even interpolating single time frames), but all artifact time frames were omitted. Channels O9 and O10 were removed because of frequent muscle artifacts in most participants, leaving 33 channels. The data were eventually segmented into artifact-free 2 s epochs and digitally band passed to 2–20 Hz. Across participants, on average there was 27.7 $\pm$ 8.0 s (25.9 $\pm$ 8.4 s) for believers (skeptics) of 33-channel artifact-free eyes-closed EEG.

For microstate analysis (Koenig et al. 2002; Lehmann et al. 1987, 2005), all momentary (potential distribution) maps at peak times of global field power (GFP) (Lehmann and Skrandies 1980) after normalization to GFP = 1 were clustered into four map topographies using k-means clustering (Pascual-Marqui et al. 1995). Across participants, the topographies of the four microstate classes explained 84.0 $\pm$ 5.1% of the total variance. The four map topographies of each participant were labeled according to the best fit microstate topography of classes A, B, C, D in a normative study (Koenig et al. 2002). The four labeled individual microstate maps of each participant were used to label the sequential momentary maps at peak times of GFP, resulting in time sequences of the four microstate classes.

An average map was computed for each microstate class for each participant. Separately for the two participant groups, an average map for each of the four microstate classes was computed across participants. The microstate map topographies were tested for global differences of the spatial potential distributions between groups using TANOVA (Strik et al. 1998). The program calculates Global Map Dissimilarity (Lehmann and Skrandies 1980) as measure of the global difference between two map topographies and establishes the exact probability of the observed difference using a randomization procedure. Channel-wise t-tests specified the spatial distributions of the differences.

The three microstate parameters of mean duration, frequency of occurrence per second, and percentage of occupied total analysis time ('coverage') were computed for each of the four microstate classes of each participant.

In addition, the frequency of GFP peaks per second was established for each microstate class and all participants.

Since microstate parameters were calculated for each 2 s epoch separately, the duration of the microstate at the

beginning and the end of an epoch were truncated, on average by 50%. We corrected the microstate mean durations by applying Eq. 1 (provided by Thomas Koenig) to the durations of each microstate class of each participant:

$$\text{duration}_{\text{corrected}}(\text{ms}) = \frac{\text{duration}_{\text{observerd}}(\text{ms}) \times (\text{occurrence} + \text{coverage})}{\text{occurrence}} \quad (1)$$

where $\text{duration}_{\text{corrected}}$ is the corrected mean duration of the microstates of class X, $\text{duration}_{\text{observed}}$ is the computed mean duration of the microstates of class X, occurrence is the number of occurrences of microstates of class X observed during the analyzed time epoch, and coverage is the fraction of time of the analyzed epoch covered by the microstates of class X.

The three microstate parameters were assessed using ANOVAs with group (believers, skeptics) as between-subject factor and microstate class (A, B, C, D) as within-subject factor.

The concatenation of the microstate classes over time ('microstate syntax') was examined as follows: The number of transitions from each of the four microstate classes to any other class (12 possibilities given the two directions of the six possible pairings of microstates), normalized by the total amount of microstate class transitions ($X \rightarrow Y$ for $X \neq Y$) was obtained for each participant. In this way, the 12 possible microstate transitions were assessed as microstate transition percentages. To examine directional asymmetries in the transitions ('directional predominance') between the six possible microstate pairs, directional predominance $X \leftrightarrow Y$ was calculated as difference of the two transition percentages between two given microstate classes $[(X \rightarrow Y) - (Y \rightarrow X)]$.

To assess the transition probabilities, ANOVAs were computed with group as between-subject factor and microstate pairing (six possibilities) as within-subject factor.

In case of statistically interesting results, correlations with the paranormal belief score were computed.

Results

Figure 1a shows the four averaged microstate map topographies for believers and for skeptics. The topographies of the obtained classes A, B, C and D resemble the topographies of previous studies (Koenig et al. 1999, 2002). The spatial distributions of the corresponding standard errors are displayed in Fig. 1b (note that isopotential lines are in steps of 1.0 units in Fig. 1a, of 0.1 units in Fig. 1b).

Figure 1c displays the *t*-values of the channel-wise *t*-tests between the map topographies of the two groups. TANOVA showed that the map topographies differed significantly between groups for microstate A ($P < 0.001$), B ($P = 0.003$), and C ($P = 0.002$) but not for microstate D. TANOVA showed that within both groups, all four microstate map topographies differed significantly from each other (*P*-values between $P < 0.01$ and $P < 0.00001$).

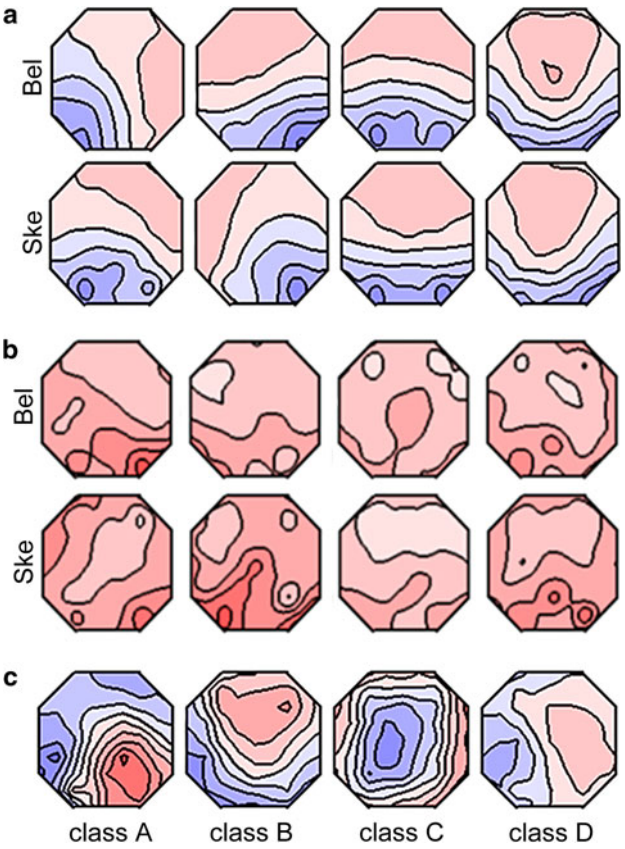

Fig. 1 The four microstate classes A–D in believers (*Bel*) and skeptics (*Ske*). **a** Mean potential distribution maps of the microstate classes of believers and skeptics, normalized for equal field power. *Red* and *blue* are the arbitrarily chosen color labels for areas of opposite polarity; isopotential lines in steps of 1.0 units. **b** Spatial distribution of standard errors of the mean; isopotential lines in steps of 0.1 units. **c** Topography of the t-values of channel-wise t-tests of differences between the potential distributions in believers and skeptics; *red*: believers higher potential than skeptics, *blue*: skeptics higher potential than believers. Iso-t-value lines in steps of $t = 1$. Head seen from above (nose up, left ear left) (Color figure online)

Viewed as channel-wise *t*-value topographies, in microstates class A, believers showed higher values right posterior ($t(\text{max}) = 4.32$), skeptics left lateral ($t(\text{max}) = -4.22$). For class B, believers had higher values right anterior ($t(\text{max}) = 3.73$), skeptics left posterior ($t(\text{max}) = -3.44$). For class C, believers had higher values in the periphery ($t(\text{max}) = 3.74$), skeptics in central areas ($t(\text{max}) = -3.81$). For class D, believers had higher values central right ($t(\text{max}) = 1.51$), skeptics in central-posterior left ($t(\text{max}) = -2.03$).

For the three microstate parameters duration, occurrence and coverage, a 2-factor ANOVA (group × microstate) revealed no main effect of group but significant group by microstate interactions for occurrence [$F(3, 81) = 4.27$;

$P = 0.007$] and coverage [$F(3.81) = 2.91$; $P = 0.039$]. Post-hoc comparisons (Table 1) revealed that microstate class B showed significant increases of occurrence and coverage in believers compared to skeptics ($P = 0.044$ and $P = 0.023$, respectively), and revealed that microstate class C showed a tendency to decreases of occurrence and coverage in believers ($P = 0.093$ and $P = 0.064$, respectively).

For class B, paranormal belief score correlated with coverage ($r = 0.43$, $N = 29$, $P = 0.019$) and showed a tendency to correlate with occurrence ($r = 0.36$, $N = 29$, $P = 0.053$) but showed no correlation with duration. For class C, paranormal belief score showed tendencies to correlate negative with coverage and occurrence ($r = -0.34$, $N = 29$, $P = 0.070$ and $r = -0.35$, $N = 29$, $P = 0.066$, respectively).

The mean frequency of GFP peaks per second across all participants decreased from microstate class A (21.44 ± 0.21 SE) to B (21.17 ± 0.22 SE) to C (20.89 ± 0.22 SE) to D (20.80 ± 0.21 SE). GFP peaks frequency of class A differed from that of classes B, C and D at $P = 0.07$, $P = 0.0002$, and $P = 0.000001$, respectively; that of class B differed from C and D at $P = 0.06$ and $P = 0.01$, respectively, while GFP peaks frequency did not differ significantly between classes C and D. The results were similar in believers and skeptics when separately examined.

For the directional predominances within the microstate syntax, a 2-factor ANOVA (group × microstate pair) revealed a significant interaction of group by microstate pair [$F(5.135) = 3.31$; $P = 0.007$]. Post-hoc analysis showed that believers differed significantly in their directional predominances for the microstate pairs A↔B, A↔C and B↔C (Table 2; Fig. 2).

This result is accounted for by the reversed directions of directional predominance for believers and skeptics as illustrated in Fig. 2 which shows that the microstate pairs A↔B, A↔C and B↔C constitute a quadruplet sequence A to C to B to A in believers and an A to B to C to A quadruplet sequence in skeptics. Figure 2 also displays the *P*-values of the separate tests of these directional predominances against the null hypothesis of no directional predominance between microstate pairs.

Across all participants, the three involved directional predominances correlated significantly with paranormal belief: For (A to C)–(C to A) $r = 0.43$, $P = 0.021$; for (C to B)−(B to C) $r = 0.56$, $P = 0.001$; and for (B to A)–(A to B) $r = 0.45$, $P = 0.015$.

Based on these findings of directional predominance in believers and skeptics, all possible quadruplets of the microstates sequences A → C→B → A, C → B→A → C and B → A→C → B ('left-rotating') as well as A → B→C → A, B → C→A → B and C → A→B → C ('right-rotating') were counted and expressed as percentages of the total number of microstates for each participant. The difference of left-rotating minus right-rotating quadruplet percentages was computed for each participant. Comparing these differences between groups, believers

Table 1 Microstate parameters

	Microstate class							
	A		B		C		D	
	Mean	SD	Mean	SD	Mean	SD	Mean	SD
Duration (ms)								
Believers	74.86	11.29	86.01	16.15	89.21	16.35	82.20	15.25
Skeptics	77.28	15.18	78.70	25.28	93.35	14.06	81.72	22.18
t ($df = 27$)	−0.48		0.91		−0.70		0.07	
P	0.64		0.37		0.49		0.95	
Occurrences/s								
Believers	2.61	0.71	3.27	0.61	3.39	0.53	3.26	0.49
Skeptics	3.00	0.79	2.64	1.00	3.81	0.77	3.12	0.80
t ($df = 27$)	–1.40		2.11		−1.74		0.58	
P	0.17		**0.044**		**0.093**		0.57	
Coverage (% time)								
Believers	19.03	5.80	26.28	4.49	28.99	5.61	25.68	5.21
Skeptics	21.65	6.21	20.08	9.05	33.75	7.66	24.53	8.02
t ($df = 27$)	−1.17		2.41		−1.93		0.47	
P	0.25		**0.023**		**0.064**		0.65	

Mean and standard deviation (SD) for 16 believers and 13 skeptics as well as tests for group differences (unpaired *t*-tests)

Bold values indicate $P < 0.05$

Table 2 Directional predominances in the microstate syntax

	Believers				Skeptics				Believers–skeptics		
	Mean	SD	t ($df = 15$)	P (H_0)	Mean	SD	t ($df = 12$)	P (H_0)	Mean diff.	t ($df = 27$)	P
A↔B	−0.51	1.41	−1.45	0.168	0.48	0.91	1.91	0.081	−0.99	−2.19	**0.037**
A↔C	0.64	1.25	2.06	0.057	−0.41	0.82	−1.78	0.101	1.05	2.60	**0.015**
A↔D	0.02	0.96	0.09	0.930	0.01	1.20	0.04	0.973	0.01	0.03	0.980
B↔C	−0.58	1.24	−1.87	0.082	0.91	1.13	2.91	**0.013**	−1.49	−3.34	**0.002**
B↔D	−0.03	1.69	−0.08	0.941	−0.21	1.37	−0.56	0.587	0.18	0.31	0.759
C↔D	0.01	1.10	−0.05	0.960	0.46	1.49	1.10	0.291	−0.44	−0.92	0.366

Mean and standard deviation (SD) of the percentages of directional predominances [X↔Y = (X → Y)–(Y → X)] for 16 believers and 13 skeptics. Test results for H_0: X↔Y = 0 are shown for each group (paired t-tests) as well as tests for group differences (unpaired t-tests)

Bold values indicate $P < 0.05$

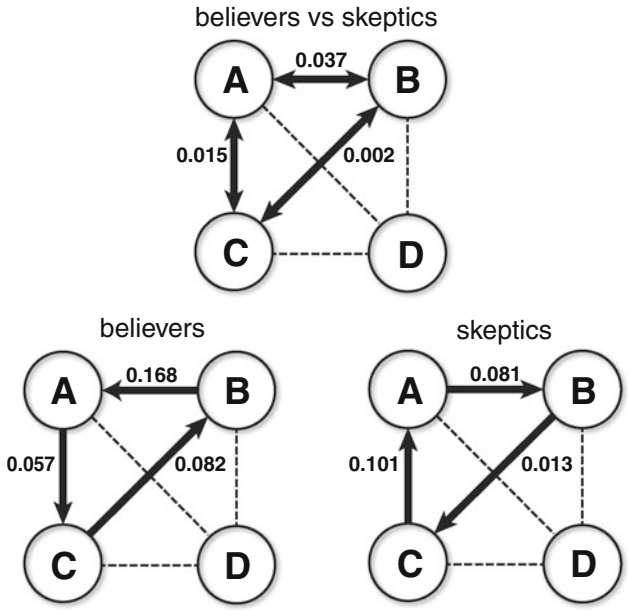

Fig. 2 Directional predominances of microstate concatenations for the 16 believers and 13 skeptics. *Letters* indicate the microstate classes A through D; *lines* indicate the six possible transitions between pairs of microstate classes. *Upper graph* Directional predominances differed significantly between believers and skeptics for the concatenation of microstates of classes A, B and C; P-values < 0.05 are listed. *Lower graphs* Directional predominances for the concatenation of the microstate classes A, B and C separately illustrated for believers and skeptics show inverted sequencing. The t-test results of the directional predominances between microstate classes versus no directional predominances are listed

tended to have a higher preference for left quadruplets than skeptics (0.67 ± 1.65% vs. −0.29 ± 0.66%; $t = 1.97$; df = 27; $P = 0.059$).

Discussion

The microstate features reflected the personality difference between believers and skeptics. Rapid spontaneous reorganization of large-scale neuronal activity, characterized by the EEG microstates, represents the brain's ability to flexibly react to and integrate various incoming information. Hence, deviations in the tuning of the spontaneous microstate parameters reflect differences in the cognitive style and thus different dispositions to interpret the environment, here expressed as belief in and skepticism of paranormal phenomena.

Microstates of class B in believers compared to skeptics showed increased occurrence; because there was no difference in duration, an increase in time coverage resulted. Class B microstates have been associated with concrete/visual imagery-type thoughts as opposed to microstate class A which has been associated with abstract thoughts (Lehmann et al. 1998, 2010). Microstate class B has been correlated with negative BOLD signals in posterior occipital regions that are dedicated to visual processing (Britz et al. 2010). The same network had previously been identified as RSN 3 by Mantini et al. (2007). Thus, the present result suggests that believers tend to spend more time with thoughts of the concrete/visual imagery-type than skeptics.

On the other hand, microstates of class C in believers compared to skeptics showed a tendency to decreased occurrence that, in the absence of a difference in duration, resulted in decreased time coverage. Microstate class C has been correlated with positive BOLD signals in the ACC, bilateral inferior frontal gyri as well as right insula (Britz et al. 2010) comparable to the regions of RSN 6 in Mantini et al. (2007). Class C microstates have been suggested to involve processing with reduced attention (Brandeis and Lehmann 1989; Koenig et al. 1999); this would suggest that believers tend to spend less time in reduced attention than skeptics.

We note that microstate classes A and B because of their higher GFP peaks frequencies imply higher neural activation levels, i.e. higher global excitation than the microstates of classes C and D.

Since a given microstate is co-determined by its preceding microstate, one could speculate on inferences of the

successive steps of cognitive processes based on the microstate syntax: In believers, a concrete thought (class B) is followed by abstraction (class A) which in turn leads to decreased attention with decreased excitation (class C), while in skeptics, an abstract thought (class A) is followed by concretization (class B) which in turn leads to decreased attention with decreased excitation (class C). Vice versa, decreased attention is followed by a concrete thought in believers and by an abstract thought in skeptics. Certainly, more research is needed to corroborate such speculative interpretations in view of the very limited knowledge on functional significance of the microstate classes.

Microstate classes A, B, and C differed significantly in topography between believers and skeptics. It is obvious that humans have more than four different types of thought, even though the number of different thought types most likely is quite limited. Our analysis forced all maps into the four standard microstate classes that were repeatedly reported as reviewed in the introduction. Hence, a given microstate class in a given individual will consist of different topographies. In general, a given microstate class must be assumed to encompass a relatively large repertoire of related processing strategies. Differences between groups in the composition of the repertoire of processing strategies of a given class will be detectable as topographic differences of microstates.

Even though the topography of a microstate class might differ to some extent between participant groups, this would not imply a fundamental difference because the class designation was imposed by the class template that optimized the assignment ensuring maximal difference to the other classes (as a consequence, the topographies of the four microstate classes differed significantly from each other). But, for the same reason, the microstate classes must imply fundamental differences in brain activity. Most importantly, the topographies assigned to their microstate classes behave in the same fashion, irrespective to individual differences, i.e., they are anticorrelated to all the other classes. As it has been well established in schizophrenia studies, the microstate parameters reveal reliable and consistent group differences across a large diversity of participants, in spite of the variety of contributing map topographies.

Microstate classes A and B displayed a significantly stronger right-hemispheric activity in believers compared to skeptics. This reflects the finding in the earlier wave frequency-oriented analysis of the same data by Pizzagalli et al. (2000) where believers compared to skeptics showed a right-shifted gravity center of brain activity in the beta-2 frequency band, confirming a hypothesized right-hemispheric functional predominance in people with tendencies to paranormal ideation (Brugger and Graves 1997; Leonhard and Brugger 1998; Pizzagalli et al. 2001).

We note that the analysis approaches of the present study and that of Pizzagalli et al. (2000) are completely different: The present analysis classifies each momentary time frame according to its topography and thereby distinguishes time epochs with different topographies. This detects changes of the functional state of the brain at a very high time resolution. Frequency decomposition is not part of the approach. On the other hand, the Fourier transformation and decomposition into 'wave' frequencies (or frequency bands) convolutes the data over time and therefore yields results that refer to the entire analyzed data. Because the two approaches examine the data from completely different viewpoints, their results will detect different aspects and thereby complement each other.

Relating paranormal belief as one of the features of schizotypal personalities to increased risk for schizophrenia (Eckblad and Chapman 1983; Meehl 1962) leads to the question whether the present results support a relation between brain mechanisms of paranormal belief and those of schizophrenia. Electrophysiological relations between schizotypy and paranormal belief have been discussed (Pizzagalli et al. 2000). However, the principal deviations of microstate parameters in schizophrenia (Irisawa et al. 2007; Kikuchi et al. 2007; Koenig et al. 1999; Lehmann et al. 2005; Strelets et al. 2003), i.e., decreased duration of classes B and D and increased occurrence of A and C were not observed in the believers. In fact, believers showed an opposing result, decreased occurrence of C. Increased occurrence of B as seen in believers had been reported only in one schizophrenia study (Kikuchi et al. 2007). The scale-free dynamics of microstates (see introduction) have been shown to depend on microstate duration (Van De Ville et al. 2010), the prominently deviant parameter in schizophrenia. Since our groups did not differ in microstate durations, this would suggest that the results represent short-term dependencies that may not be visible in fMRI, i.e., after strong temporal low-pass filtering. Microstate syntax fundamentally differed between the present study and findings in schizophrenia: While believers and skeptics showed inverted sequencing between microstate classes A, B, and C, schizophrenics and normals showed inverted sequencing between microstate classes A, C, and D (Lehmann et al. 2005). In sum, the present EEG microstate analysis showed very little support for electrophysiological similarities between paranormal beliefs and schizophrenia; this would agree with the notion that paranormal belief may exist without tendencies to psychosis (Goulding 2004; McCreery and Claridge 2002).

Acknowledgment We thank Dr. Diego Pizzagalli for his help with the data collection.

References

Brandeis D, Lehmann D (1989) Segments of ERP map series reveal landscape changes with visual attention and subjective contours. Electroencephalogr Clin Neurophysiol 73:507–519

Britz J, Landis T, Michel CM (2009) Right parietal brain activity precedes perceptual alternation of bistable stimuli. Cereb Cortex 19:55–65

Britz J, Van De Ville D, Michel CM (2010) BOLD correlates of EEG topography reveal rapid resting-state network dynamics. Neuroimage 52:1162–1170

Brugger P, Graves RE (1997) Right hemispatial inattention and magical ideation. Eur Arch Psychiatry Clin Neurosci 247:55–57

Chatrian G, Lettich E, Nelson P (1988) Modified nomenclature for the "10%" electrode system. J Clin Neurophysiol 5:183–186

Eckblad M, Chapman LJ (1983) Magical ideation as an indicatior of schizotypy. J Consult Clin Psychol 51:215–225

Goulding A (2004) Schizotypy models in relation to subjective health and paranormal beliefs and experiences. Pers Individ Dif 37:157–167

Irisawa S, Isotani T, Yagyu T, Morita S, Nishida K, Yamada K, Yoshimura M, Okugawa G, Nobuhara K, Kinoshita T (2006) Increased omega complexity and decreased microstate duration in nonmedicated schizophrenic patients. Neuropsychobiology 54:134–139

Kikuchi M, Koenig T, Wada Y, Higashima M, Koshino Y, Strik W, Dierks T (2007) Native EEG and treatment effects in neuroleptic-naïve schizophrenic patients: time and frequency domain approaches. Schizophr Res 97:163–172

Koenig T, Lehmann D, Merlo MCG, Kochi K, Hell D, Koukkou M (1999) A deviant EEG brain microstate in acute, neuroleptic-naive schizophrenics at rest. Eur Arch Psychiatry Clin Neurosci 249:205–211

Koenig T, Prichep L, Lehmann D, Sosa PV, Braeker E, Kleinlogel H, Isenhart R, John ER (2002) Millisecond by millisecond, year by year: normative EEG microstates and developmental stages. Neuroimage 16:41–48

Lehmann D, Skrandies W (1980) Reference-free identifiation of components of che checkerboard-evoked multichannel potential fields. Electroencephalogr Clin Neurophysiol 48:609–621

Lehmann D, Ozaki H, Pal I (1987) EEG alpha map series: brain micro-states by space-oriented adaptive segmentation. Electroencephalogr Clin Neurophysiol 67:271–288

Lehmann D, Strik WK, Henggeler B, Koenig T, Koukkou M (1998) Brain electric microstates and momentary conscious mind states as building blocks of spontaneous thinking: I. Visual imagery and abstract thoughts. Int J Psychophysiol 29:1–11

Lehmann D, Faber PL, Galderisi S, Herrmann WM, Kinoshita T, Koukkou M, Mucci A, Pascual-Marqui RD, Saito N, Wackermann J, Winterer G, Koenig T (2005) EEG microstate duration and syntax in acute, medication-naive, first-episode schizophrenia: a multi-center study. Psychiatry Res Neuroimaging 138: 141–156

Lehmann D, Pascual-Marqui RD, Strik WK, Koenig T (2010) Core networks for visual-concrete and abstract thought content: a brain electric microstate analysis. Neuroimage 49:1073–1079

Leonhard D, Brugger P (1998) Creative, paranormal, and delusional thought: a consequence of right hemisphere semantic activation? Neuropsychiatry Neuropsychol Behav Neurol 11:177–183

Mantini D, Perrucci MG, Gratta DC, Romani GL, Corbetta M (2007) Electrophysiological signatures of resting state networks in the human brain. Proc Natl Acad Sci USA 104:13170–13175

McCreery C, Clardige G (2002) Healthy schizotypy: the case of out-of-the-body experiences. Pers Individ Dif 32:141–154

Meehl PE (1962) Schizotaxia, schizotypy, schizophrenia. Am Psychol 17:827–838

Mischo J, Boller E, Braun G (1993) Fragebogenuntersuchung zur Erfassung von okkulten Glaubenshaltungen und Merkmalen schizotypischer Verarbeitung. The Institute for Frontier Areas of Psychology and Mental Health, Freiburg i. Br, Germany

Mohr C, Michel CM, Lantz G, Ortigue S, Viaud-Delmon I, Landis T (2005) Brain state-dependent functional hemispheric specialization in men but not in women. Cereb Cortex 15:1451–1458

Müller TJ, Koenig T, Wackermann J, Kalus P, Fallgatter A, Strik W, Lehmann D (2005) Subsecond changes of global brain state in illusory multistable motion perception. J Neural Transm 112:1435–1463

Musso F, Brinkmeyer J, Mobascher A, Warbrick T, Winterer G (2010) Spontaneous brain activity and EEG microstates. A novel EEG/fMRI analysis approach to explore resting-state networks. NeuroImage 52:1149–1161

Pascual-Marqui RD, Michel CM, Lehmann D (1995) Segmentation of brain electrical activity into microstates: model estimation and validation. IEEE Trans Biomed Eng 42:658–665

Pizzagalli D, Lehmann D, Gianotti L, Koenig T, Tanaka H, Wackermann J, Brugger P (2000) Brain electric correlates of strong belief in paranormal phenomena: intracerebral EEG source and regional omega complexity analyses. Psychiatry Res Neuroimaging 100:139–154

Pizzagalli D, Lehmann D, Brugger P (2001) Lateralized direct and indirect semantic priming effects in subjects with paranormal experiences and beliefs. Psychopathology 34:75–80

Strelets V, Faber PL, Golikova J, Novototsky-Vlasov V, Koenig T, Gianotti LRR, Gruzelier JH, Lehmann D (2003) Chronic schizophrenics with positive symptomatology have shortened EEG microstate durations. Clin Neurophysiol 114:2043–2051

Strik WK, Fallgatter AJ, Brandeis D, Pascual-Marqui RD (1998) Three dimensional tomography of event-related potentials during response inhibition: evidence for phasic frontal lobe activation. Electroencephalogr Clin Neurophysiol 108:406–413

Van De Ville D, Britz J, Michel CM (2010) EEG microstate sequences in healthy humans at rest reveal scale-free dynamics. Proc Natl Acad Sci USA 107:18179–18184

Wackermann J, Lehmann D, Michel CM, Strik WK (1993) Adaptive segmentation of spontaneous EEG map series into spatially defined microstates. Int J Psychophysiol 14:269–283